

# Immunolocalization of Endogenous Indole-3-Acetic Acid and Abscisic Acid in the Shoot Internodes of *Fargesia yunnanensis* Bamboo during Development

Shuguang Wang<sup>1</sup>

*College of Life Science, Southwest Forestry University, Kunming, Yunnan 650224, P.R. China*

Yongpeng Ma<sup>1</sup>

*Key Laboratory for Plant Diversity and Biogeography of East Asia, Kunming Institute of Botany, Chinese Academy of Sciences, Kunming, Yunnan 650201, P.R. China*

Chengbin Wan

*College of Foreign Languages, Southwest Forestry University, Kunming, Yunnan 650224, P.R. China*

Chungyun Hse

*Southern Research Station, USDA Forest Service, Pineville, LA 71360*

Todd F. Shupe

*School of Renewable Natural Resources, Louisiana State University Agricultural Center, Baton Rouge, LA 70803*

Yujun Wang

*Bamboo Research Institute, Nanjing Forestry University, Nanjing, Jiangsu 210037, P.R. China*

Changming Wang<sup>2</sup>

*College of Life Science, Southwest Forestry University, Kunming, Yunnan 650224, P.R. China*

**ADDITIONAL INDEX WORDS.** bamboo shoot, internode elongation, endogenous hormone, immunolabeling

**ABSTRACT.** The Bambusoideae subfamily includes the fastest-growing plants worldwide, as a consequence of fast internode elongation. However, few studies have evaluated the temporal and spatial distribution of endogenous hormones during internode elongation. In this paper, endogenous indole-3-acetic acid (IAA) and abscisic acid (ABA) were detected in different developmental internodes during shoot elongation by immunolocalization. Immunohistochemistry showed that IAA was mainly present in the shoot apex, leaf sheath primordia, parenchymal cells, and vascular tissues. During internode elongation and maturation, the IAA signals decreased significantly and then increased slightly, with the weakest signals observed in the rapidly elongating internode. Based on immunogold localization, most IAA signals were detected in the cytoplasm and nuclei of both parenchymal and fiber cells, and few signals were detected in cell walls in the unelongated and elongating internodes. After the completion of internode elongation, additional IAA signals were detected in the secondary walls of both parenchymal and fiber cells. Immunohistochemical localization of ABA showed that ABA signals decreased with internode elongation and maturation, with the weakest signal observed in the internodes of 3-month-old shoots. In addition, few ABA signals were detected in the shoot apex. The strongest IAA and ABA signals in unelongated internodes suggested that both hormones participated in the mediation of internode differentiation but not in the rapid elongation. Moreover, IAA was involved in secondary cell wall deposition.

Phytohormones are small molecules that are derived from secondary metabolism and play key roles in shaping the plant architecture (Santner and Estelle, 2009). The presence and effect of some of these hormones have been recognized for more than a century (Jaillais and Chory, 2010). IAA is the most abundant naturally occurring auxin and is involved in many aspects of plant growth and development, such as cell division and elongation, differentiation, tropism, apical dominance,

senescence, abscission, and flowering (Chudasama and Thaker, 2007; Mano and Nemoto, 2012; Teale et al., 2006; Woodward and Bartel, 2005). To date, a large number of studies have focused on the role of auxin in rhizogenesis (Dong et al., 2012, 2014; Falasca et al., 2004; Gangopadhyay et al., 2010; Ludwig-Muller et al., 2005; Xuan et al., 2008), embryogenesis and development (Chen et al., 2010; Thomas et al., 2002; Zhang et al., 2015), and floral induction (Hou and Huang, 2005).

ABA is a small molecule that is naturally generated in plants and was named for its propensity to accumulate in dry, mature leaves (Moore, 1989). After ABA was first identified, it quickly became accepted as one of the five major phytohormones (Peng et al., 2006). ABA has major roles in plant responses to drought or osmotic stress, cold stress, wounding, and pathogen assault (Mauch-Mani and Mauch, 2005; Verslues and Zhu, 2005;

Received for publication 17 May 2016. Accepted for publication 15 Aug. 2016. This research was fully funded by the Advanced and Characteristic Key Biological Disciplines of Yunnan Province (50097505), the Science Foundation of Yunnan Province (2015FB150), and the China National Science Foundation (31560196).

<sup>1</sup>These authors contributed equally to this work.

<sup>2</sup>Corresponding author. E-mail: 253692357@qq.com.

Yamaguchi-Shinozaki and Shinozaki, 2005). ABA also functions in seed dormancy and germination (Gubler et al., 2005). In addition, ABA has also been reported to participate in sugar signaling (Arenas-Huertero et al., 2000; Brocard-Gifford et al., 2004; Çakir et al., 2003; Carrari et al., 2004; Finkelstein and Gibson, 2002; Rook et al., 2001; Smeeckens, 2000) and to affect the distribution of sucrose and protons across the plasmalemma in the pea (*Pisum sativum*) mesophyll (Opaskornkul et al., 1999). Furthermore, ABA is preferentially localized in phloem cells (Peng et al., 2003; Zhang et al., 1999, 2001a, 2001b). Therefore, ABA may play some “positive” role during plant development by participating in the regulation of the distribution of assimilation, in addition to its well-known function as a “negative hormone” (Peng et al., 2006).

Bamboos (Poaceae, Bambusoideae) are the fastest-growing plants worldwide, and their culms can reach their final height within relatively short periods of 2 to 4 months (Magel et al., 2005). Although some research has been conducted to assess bamboo growth (Cui et al., 2012; Peng et al., 2013), the mechanism responsible for the fast growth rate remains unknown. Plant hormones play an important role in the regulation and coordination of cell proliferation and elongation (Wang et al., 2015). However, to date, very few studies have focused on endogenous hormones in bamboos or on endogenous hormone contents in moso bamboo (*Phyllostachys pubescens*) (Ding, 1997; Wang et al., 2015). Most of the reported studies have been quantitative analyses of phytohormones using various analytical methods. However, even the most advanced methods must use a certain amount of material, and the concentration of phytohormones in the target site and not the whole tissue could reflect activity levels (Dong et al., 2012). Therefore, immunohistochemical localization is an important technique for evaluating endogenous hormones during the rapid growth of bamboos. In addition, information regarding the sites of IAA and ABA storage and transport, and the characteristics of their dynamic spatial changes during shoot elongation are quite limited, necessitating further investigations. The subcellular localization of endogenous IAA and its role in shoot elongation remain unclear. In this paper, the spatial distribution patterns of endogenous IAA and ABA, and their dynamic changes during shoot elongation of *Fargesia yunnanensis* were investigated. The correlation between phytohormones and bamboo internode elongation was also analyzed. The findings presented will provide more

information regarding the regulation of endogenous IAA and ABA during shoot internode elongation.

## Materials and Methods

**PLANT MATERIALS.** *Fargesia yunnanensis* belongs to sympodial bamboos with a long-necked pachymorph rhizome (pseudorhizomes) that grows to a height of  $\approx 10$  m. Shoot growth is usually initiated in September. Among the internodes assessed herein, the first (labeled as internode 1), third (labeled as internode 3), and fifth (labeled as internode 5) aboveground internodes, the apex portion of the 0.5-month-old shoot, internode 1 of the 1-month-old culms, and internode 1 of the 3-month-old culms were obtained and used as samples for the immunohistochemical localization of IAA and ABA. All samples were collected in Sept. and Oct. 2013. The characteristics of the sampled internodes are presented in Table 1.

**PARAFFIN AND ULTRATHIN SECTIONS.** The middle portions of all chosen internodes were cut into  $\approx 3\text{-mm}^3$  blocks, which were immediately prefixed in a 2% (wt/v) aqueous solution of 1-ethyl-3(3-dimethyl-aminopropyl)-carbodiimide hydrochloride (Sigma-Aldrich, St. Louis, MO) at 4 °C for  $\approx 8$  h and then postfixed in glutaraldehyde fixative containing 2% paraformaldehyde and 2.5% glutaraldehyde in 0.025 M phosphate buffer solution (PBS, pH 7.2) at 4 °C. For the microscopic observation, paraffin embedding was employed. Seven-micrometer-thick paraffin sections were cut using a rotary microtome. To determine the subcellular localization of endogenous IAA, the samples were dehydrated in a graded ethanol series and then embedded in Lowicryl K4M Resin (Polysciences, Warrington, PA) at  $-20$  °C. The resins were polymerized by long-wavelength ultraviolet irradiation for 48 h. Semithin sections were cut to examine the location of vascular bundles, and then ultrathin sections (60 nm) were cut with a diamond knife on an ultramicrotome and mounted on nickel grids (100 mesh) with Formvar (Zhongjingkeyi, Beijing, China).

**LOCALIZATION OF IAA.** The tissue-specific immunolocalization of endogenous IAA was performed as follows. After washing three times with TBST<sup>Ⓢ</sup> solution [(0.05 M pH 7.4 Tris-HCl buffer, 0.15 M NaCl) solution + 0.3% (v/v) Triton X-100 (Solarbio, Beijing, China)], the sections were incubated for 45 min in a blocking solution [5% (wt/v) bovine serum albumin (BSA; Sigma-Aldrich) and 1.5% (wt/v) glycine in TBST<sup>Ⓢ</sup> solution] and then incubated overnight at 4 °C with anti-IAA antibodies (Agdia,

Table 1. Morphological characteristics of the sampled *Fargesia yunnanensis* internodes by microscopy and transmission electron microscopy.

Sample	Position	Age (mo.)	Morphological characteristics
Shoots (27 cm in height)	Apex and internodes close to the apex	0.5	Unelongated, soft, faint yellow, and enveloped entirely by purple culm sheaths.
	Internode 5	0.5	Unelongated, soft, light yellow, 1.0 cm long, 0.5 cm in diameter, and enveloped entirely by purple culm sheaths.
	Internode 3	0.5	Elongation initiated, soft, light yellow, 2.0 cm long, 1.4 cm in diameter, and enveloped entirely by culm sheaths.
	Internode 1	0.5	Elongating rapidly, hard, light yellow, 5.0 cm long, 2.5 cm in diameter, and enveloped entirely by purple culm sheaths.
Shoots (85 cm in height)	Internode 1	1	Internode elongation completed and maturation initiated. Hard, yellow and green, 8.0 cm long, 2.2 cm in diameter, and enveloped entirely by purple culm sheaths.
Culms (9.76 m in height)	Internode 1	3	Mature, hard, bright green, 7.5 cm long, 2.4 cm in diameter, and enveloped by greyish-white culm sheaths.

Elkhart, IN) diluted 1:100 in blocking solution. Subsequently, the sections were incubated for 6 h at room temperature with gold-labeled goat antimouse immunoglobulin G (IgG, 11 nm in diameter) (Abcam, Cambridge, UK) diluted 1:50 in blocking solution. After washing five times with TBST<sup>®</sup> [2.5% (wt/v) BSA in TBST<sup>®</sup> solution] and double-distilled (dd) H<sub>2</sub>O for 10 min, the sections were stained with a silver staining solution [1.7% (wt/v) hydroquinone, 0.05% (wt/v) silver nitrate, 2.55% (wt/v) citric acid, 2.35% (wt/v) sodium citrate, 0.3% (wt/v) gelatin 40% (v/v) ddH<sub>2</sub>O] in the dark for ≈10–15 min. As the color developed (15–20 min) in sections, they were rinsed with ddH<sub>2</sub>O and photographed. The sections were examined under a converted fluorescence microscope (E400; Nikon, Tokyo, Japan).

The subcellular immunolocalization of endogenous IAA was performed according to the following procedure. Ultrathin sections were incubated in a blocking solution at room temperature for 30 min and then incubated overnight at 4 °C with anti-IAA antibodies (Agdia) diluted 1:100 in blocking solution. After three 5-min washes in TBST<sup>®</sup>, the sections were incubated for 1 h at room temperature with gold-labeled goat antimouse Immunoglobulin G diluted 1:50 in blocking solution. Finally, the sections were rinsed consecutively with TBST<sup>®</sup> and ddH<sub>2</sub>O, stained with 2% uranyl acetate and 4% lead citrate, and examined under a transmission electron microscope (TEM; JEM-1400; JEOL, Tokyo, Japan). The controls were obtained by omitting the anti-IAA antibody to verify the specificity of the anti-IAA antibody.

The distribution of IAA in different cells was revealed by the number of immunogold particles. To illustrate the distribution quantitatively, the density of the gold particles in different parenchymal cells was measured (Dong et al., 2014). For each internode sample, 15 cells were randomly selected, and the number of particles per 5 μm<sup>2</sup> was counted. The mean values derived from the experiments were compared by multiple comparisons using the least significant difference method.

**LOCALIZATION OF ABA.** The tissue-specific immunolocalization of endogenous ABA was performed as follows. The dewaxed paraffin sections were incubated in a blocking solution at room temperature for 60 min and then incubated overnight at 4 °C with anti-ABA antibodies (MAC 252; Abcam) diluted 1:200 in blocking solution. After five 3-min washes in TBST<sup>®</sup>, the sections were incubated with fluorescein isothiocyanate-labeled goat antimouse IgG (Sigma-Aldrich) diluted 1:50 in blocking solution in the dark for 45 min at room temperature. The sections were rinsed with TBST<sup>®</sup> (three 3-min washes), and examined under a fluorescence microscope. The anti-ABA antibody was omitted as a control to verify its specificity.

**ANATOMICAL OBSERVATIONS OF INTERNODE DEVELOPMENT.** Hoechst 33342 stain was used to visualize nuclei during cell development (Elbaz et al., 2002; Gorpenchenko et al., 2012). In this paper, the Hoechst stain was diluted to 1 μg·mL<sup>-1</sup> in Dulbecco's PBS (DPBS; Dulbecco and Vogt, 1954) containing 8 mM

sodium phosphate, 2 mM potassium phosphate, 140 mM sodium chloride, and 10 mM potassium chloride (pH 7.4). After dewaxing and rehydration, the paraffin sections were washed and then stained for 10 min before being washed with DPBS. After staining, all sections were examined using a converted fluorescence microscope.

## Results

**IMMUNOLocalIZATION OF IAA.** A strong IAA signal was localized in the bamboo shoot apex, including the shoot sheath primordia, apical meristem, and young shoot sheaths (Fig. 1A). In the differentiating internodes close to the shoot apex, there were also strong IAA signals detected in cells around the vascular tissues, but few signals in the pith cells (Fig. 1B). The subcellular localization indicated that the IAA signals were mainly detected in the nuclei, cytoplasm, and a few in the cell wall but and few in vacuoles (Fig. 1C and D).

In the unelongated internode (internode 5 of 0.5-month-old plants), the IAA signal was concentrated in the cells surrounding the xylem and phloem (Fig. 2A). In addition, a strong IAA signal was also detected in companion cells of the phloem. The cytoplasm of the parenchymal cells between the vascular bundles and between the xylem and phloem also exhibited a strong IAA signal. Similarly, IAA was also mainly localized in the cytoplasm of fibers, with very little detected in the vacuoles and fiber walls (Fig. 2B and C). In parenchymal cells, the IAA signal was mainly located in the nucleus and cytoplasm, and very little signal was observed in the vacuoles and starch grains (Fig. 2D).

Following the initiation of internode elongation (internode 3 of 0.5-month-old plants), the strong IAA signals were mainly

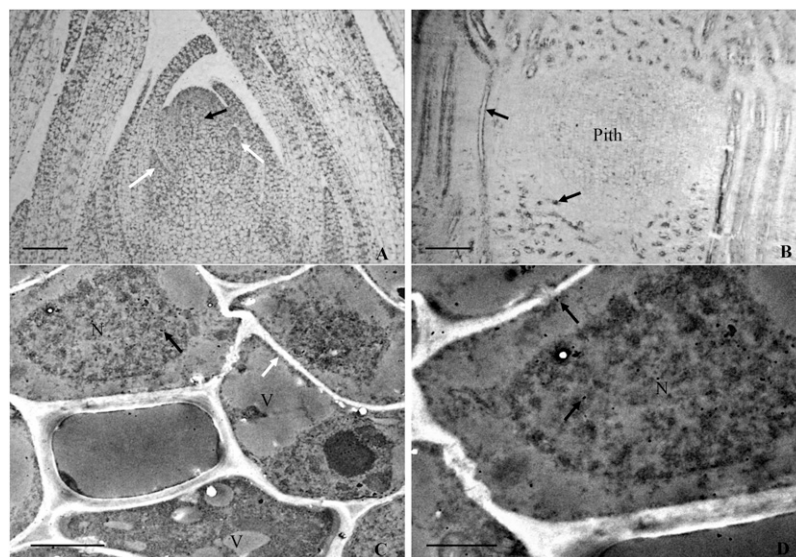


Fig. 1. Localization of indole-3-acetic acid (IAA) at the top of *Fargesia yunnanensis* shoots. (A) Immunohistochemical localization at the shoot tip, showing the strong IAA signal in the apical meristem (black arrow), sheath primordia (white arrows), and new sheaths. The internodes between different sheath primordia were still undifferentiated; bar = 40 μm. (B) Immunohistochemical localization in the new differentiated internode close to the shoot apex, showing the strong IAA signal in the cells surrounding the vascular bundles (black arrow) and the weak signal in the pith cells; bar = 100 μm. (C and D) Subcellular localization in fiber cells, showing most of the gold particles (black arrows) in the cytoplasm and nuclei (N), a few in cell walls and a few in vacuoles. The cytoplasm was pressed against the cell wall due to enlargement of the vacuoles [V (white arrow)]; (C) bar = 2 μm, (D) bar = 1 μm.

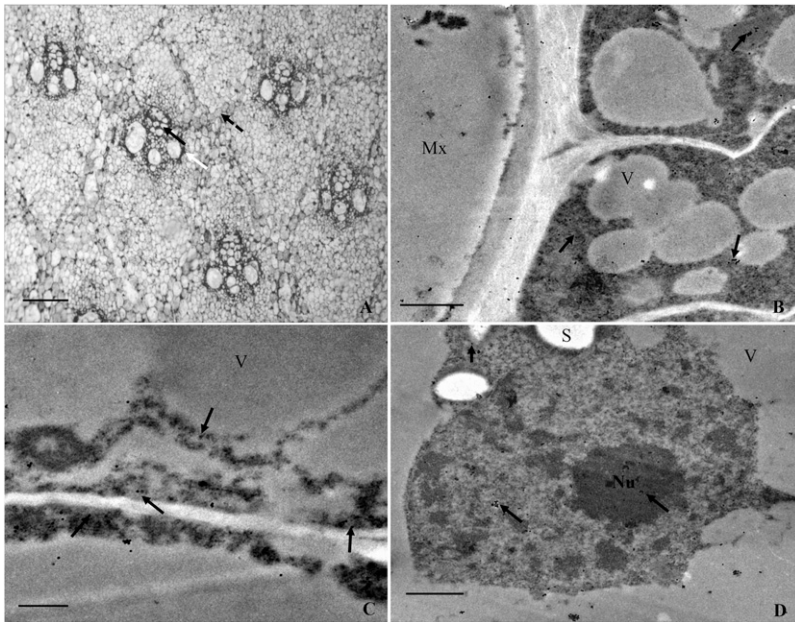


Fig. 2. Localization of indole-3-acetic acid (IAA) in internode 5 of *Fargesia yunnanensis* shoots. (A) Immunohistochemical localization in a transverse section, showing strong IAA signals in companion cells (black arrow) and parenchymal and fiber cells surrounding the xylem and phloem (white arrow). IAA was also detected in parenchymal cells between vascular bundles (dotted arrow); bar = 40  $\mu\text{m}$ . (B and C) Immunogold localization of IAA in fibers adjacent to the metaxylem, showing more gold particles (black arrows) in the cytoplasm and few in the vacuoles (V). Vacuolation of fibers increased significantly compared with that in the internode close to the shoot apex; (B) bar = 1  $\mu\text{m}$ , (C) bar = 0.5  $\mu\text{m}$ . (D) Immunolocalization of IAA in parenchymal cells, showing that most gold particles (black arrows) were located in the nucleus and nucleolus (Nu), while few were observed in the starch grains (S) and vacuoles; bar = 1  $\mu\text{m}$ .

detected in the cells surrounding the vascular tissues, cytoplasm, and nuclei of parenchymal cells and phloem companion cells (Fig. 3A). The metaxylem vessels also displayed a strong IAA signal in the residual cytoplasm and nuclei. In the fibers, most IAA signals were mainly concentrated in the cytoplasm, which was pressed against the fiber walls by the enlarging vacuoles (Fig. 3B). Similarly, a large number of gold particles was detected in the nuclei and cytoplasm of parenchymal cells, which was also pressed against the walls due to the increased vacuolation (Fig. 3C and D). Few gold particles could be detected in the vacuoles and walls of either fiber or parenchymal cells at this stage.

During the rapid internode elongation stage (internode 1 of 0.5-month-old shoots), weak IAA signals were detected in the walls of parenchymal and fiber cells based on histology (Fig. 4A). The subcellular localization revealed a few gold particles in the cytoplasm close to the cell wall in both fiber and parenchymal cells, and few in the vacuoles (Fig. 4B and C).

Following the completion of internode elongation (internode 1 of 1-month-old shoots), the strong IAA signals were mainly localized in the fiber walls based on immunohistochemical localization. In addition, the fiber and parenchymal cells adjacent to the xylem and phloem also exhibited a strong IAA signal (Fig. 5A). The subcellular localization of IAA showed that the strong signals were mainly detected in the fiber walls at this stage (Fig. 5B). After 3 months, elongation of the entire culm was completed. The endogenous IAA was mainly localized in the walls of the parenchymal cells between or around the vascular elements (Fig. 6A). The subcellular localization of IAA revealed a large number of gold particles localized in the

metaxylem vessel walls and secondary fiber walls (Fig. 6B and C). Similarly, the walls of the parenchymal cells between the phloem and xylem also displayed a large number of gold particles (Fig. 6D).

A statistical analysis of the density of the gold particles in the parenchymal cells of different internodes is shown in Fig. 7. The number of gold particles decreased significantly with the rapid elongation of the internode. However, a trend toward a slight increase was observed during secondary cell wall deposition, although this difference was not significant. This result showed that the rapidly elongating internode had the lowest IAA concentration, which was coincident with the immunohistochemical localization in internode 1 of 0.5-month-old shoots (Fig. 4A). This result suggested that the elongating internode had the lowest content of IAA.

**IMMUNOLocalIZATION OF ABA.** Immunolocalization of ABA was also performed in the shoot apex and internodes at different developmental stages. Figure 8A shows an extremely weak ABA signal in the longitudinal section of the shoot apex. However, a strong ABA signal was detected in the vascular tissues of internode 5 of 0.5-month-old shoots (unelongated), including the companion cells of the phloem and the cells surrounding the vascular elements (Fig. 8B). In parenchymal cells, ABA accumulation was mainly detected

in nuclei, cytoplasm, and walls (Fig. 8C). With the initiation of internode elongation, the ABA signal also weakened and became concentrated mainly in the parenchymal, cortical, and companion cells of the phloem (Fig. 8D–F). The strong ABA signal in the parenchymal cells between vascular bundles and in vascular tissues implied that these cells were the main storage pool of ABA. Few signals were detected in the cytoplasm of fibers. In addition, the ABA signal was also detected in the residual cytoplasm of metaxylem vessels (Fig. 8D). As internode 1 of 0.5-month-old shoots rapidly elongated, the ABA signal continued to weaken and was mainly detected in the vascular tissues, including the residual nuclei and companion cells (Fig. 8G). When internode elongation ceased completely, the ABA signal weakened further (Fig. 8H). Finally, almost no signals could be detected following the completion of culm elongation (Fig. 8I).

**DYNAMIC CHANGES IN ANATOMICAL CHARACTERISTICS WITH INTERNODE DEVELOPMENT.** The anatomical characteristics of internodes were evaluated during elongation, including the developmental characteristics of fiber and parenchymal cells (Fig. 9). In the internode close to the shoot apex, most parenchymal and fiber cells displayed prominent nuclei, according to observations of the longitudinal sections (Fig. 9A). Fiber elongation and parenchymal cell division could be observed in this internode, and did not produce significant internode elongation. Similarly, the longitudinal section of internode 5 (unelongated) of 0.5-month-old shoots revealed that many parenchymal cells and their nuclei adjoined one another, which was mainly due to the rapid divisions (Fig. 9B). Therefore, the rapid division of parenchymal cells was the main characteristic observed before rapid internode elongation. As the internode rapidly

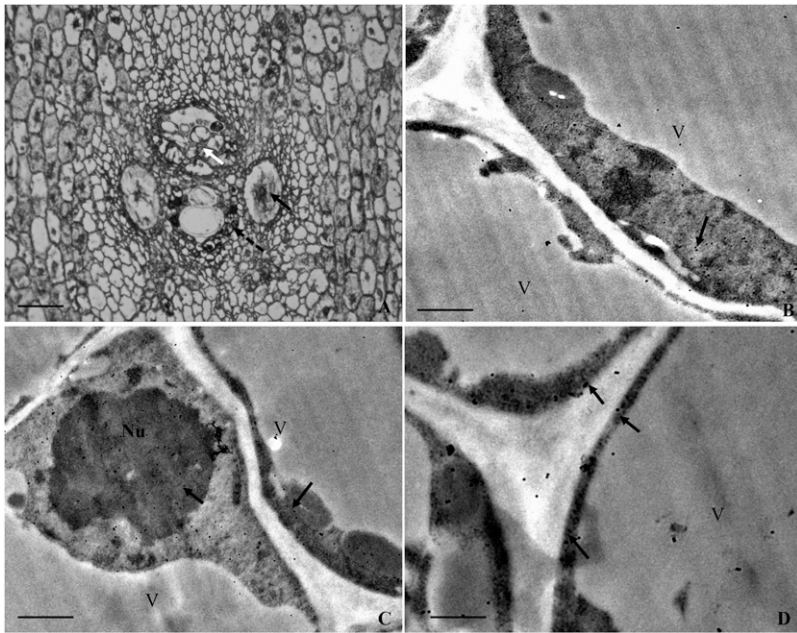


Fig. 3. Localization of indole-3-acetic acid (IAA) during elongation initiation of internode 3 in *Fargesia yunnanensis* shoots. (A) Immunohistochemical localization in the transverse section, showing strong IAA signals in the companion cells (white arrow), fiber cells surrounding the xylem and phloem (dotted arrow), and parenchymal cells between the vascular bundles. A strong IAA signal was also detected in the nucleus and cytoplasm of the vessel cells (black arrow); bar = 1  $\mu$ m. (B) Gold particles were located mainly in the cytoplasm (black arrow) of parenchymal cell. The cytoplasm was completely pressed against the cell wall by the vacuole (V); bar = 1  $\mu$ m. (C and D) Gold particles (black arrows) were also mainly detected in the cytoplasm and nuclei of fibers, while a few were observed in cell walls and vacuoles. Similarly, the cytoplasm and the residual nuclei were also pressed against the fiber walls. The nucleolus (Nu) also displayed strong IAA signals; (C) bar = 2  $\mu$ m, (D) bar = 1  $\mu$ m.

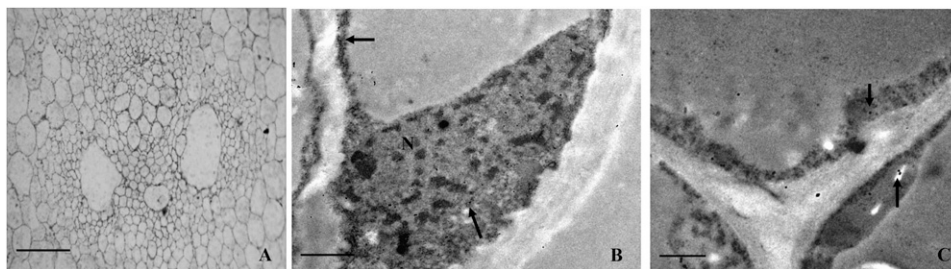


Fig. 4. Localization of indole-3-acetic acid (IAA) in internode 1 of *Fargesia yunnanensis* shoots, showing weaker IAA signals compared with the previous elongation stage. (A) Immunohistochemical localization of IAA in a transverse section, showing a faint signal in the vascular bundle; bar = 20  $\mu$ m. (B) Immunogold localization of IAA in parenchymal cells. The gold particles (black arrows) were mainly detected in the cytoplasm and nucleus (N) close to the wall; bar = 1  $\mu$ m. (C) Immunogold localization of IAA in fiber cells. Similar to parenchymal cells, the weak IAA signal (black arrows) was mainly localized in the cytoplasm close to the cell wall, with very little observed in the fiber walls; bar = 0.5  $\mu$ m.

elongated, long and short parenchymal cells began to form, and only a few parenchymal cell nuclei could be observed (Fig. 9C). The fiber cells also elongated significantly compared with Fig. 9A. Therefore, elongation of parenchymal and fiber cells was the main characteristic of rapid internode elongation. After the completion of internode elongation, long and short cells formed, and few nuclei were observed in the longitudinal section (Fig. 9D). Significant pits could be observed in the lateral walls of the parenchymal cells, which implied that secondary wall deposition occurred during this stage. Figures 5 and 6 also show secondary wall deposition in

parenchymal and fiber walls. Therefore, secondary wall deposition was the prominent characteristic after internode elongation.

To verify the specificity of the anti-IAA and anti-ABA antibodies, the primary antibodies were omitted in a control reaction. The results showed very little IAA (Fig. 10A and B) and ABA (Fig. 10C) signal, indicating that the method and the primary antibodies were reliable.

## Discussion

IAA and ABA are two of the “classic” plant hormones, which are known to regulate myriad aspects of plant growth and development (Rock and Sun, 2005). As the fastest-growing plant in the world, the height of bamboo grasses relies on the elongation of internodes, which is achieved by the activity of intercalary meristems, but not by the apical meristem. Growth begins and ends in different internodes from base to tip (Liese and Köhl, 2015). Therefore, a specific distribution of endogenous hormones can be anticipated in the fast-growing shoots.

**LOCALIZATION OF IAA AND INTERNODE ELONGATION.** By immunohistochemical localization, stronger IAA signals were present in the shoot apex, sheath primordia, and unelongated internodes compared with the rapidly elongating internodes. It is generally accepted that IAA is synthesized in the shoot apex and young leaves and then transported downward to the maturing stem and roots via a polar transport system (Ljung et al., 2001; Vieten et al., 2007), leading to the apical dominance of the plants. Unlike other plants, the fast growth of bamboo shoots does not rely on the activity of the apical meristem. In contrast, their apical meristems end plant functions during vertical growth, and no new internodes are produced after aboveground germination of the shoots. The sheath primordia in the shoot apex also develop during the final stage of

this growth phase, at a time much later than those of the lower internodes. The apex of the growing bamboo shoots has also been cut off in the wild, and elongation of the remaining internodes remained unaffected. Therefore, the IAA in the elongating internodes should be transported from the attached mature bamboos, but not the nonfunctional shoot apex.

In addition, the young bamboo shoot is devoid of photosynthetic activity and is completely parasitic toward mature bamboo culms (Su, 1965). Wang et al. (2016) considered bamboo shoot buds and shoots as the main sink tissue for starch storage. The young shoots receive carbohydrates from

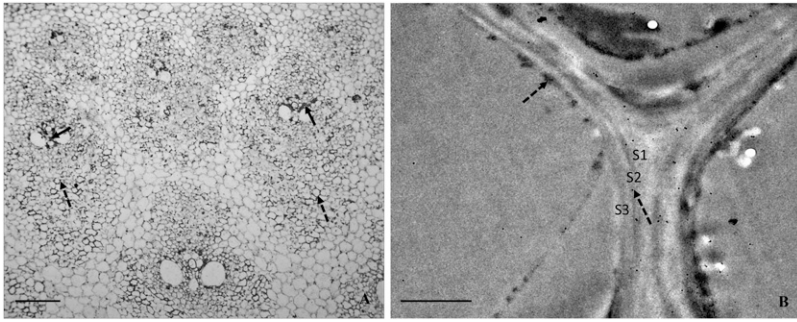


Fig. 5. Localization of indole-3-acetic acid (IAA) in internode 1 of 1-month-old *Fargesia yunnanensis* shoots. The elongation of internode 1 had ceased at this time. Secondary wall deposition occurred in the fiber walls. (A) Immunohistochemical localization of IAA in the transverse section. IAA signals were mainly detected in the cells surrounding the phloem and xylem (black arrows) and the fiber walls (dotted arrows); bar = 40  $\mu$ m. (B) Additional gold particles were localized in the fiber walls, and a few were observed in the cytoplasm adjacent to the walls (black arrows). At least three layers of secondary walls (S1, S2, and S3) were deposited; bar = 1  $\mu$ m.

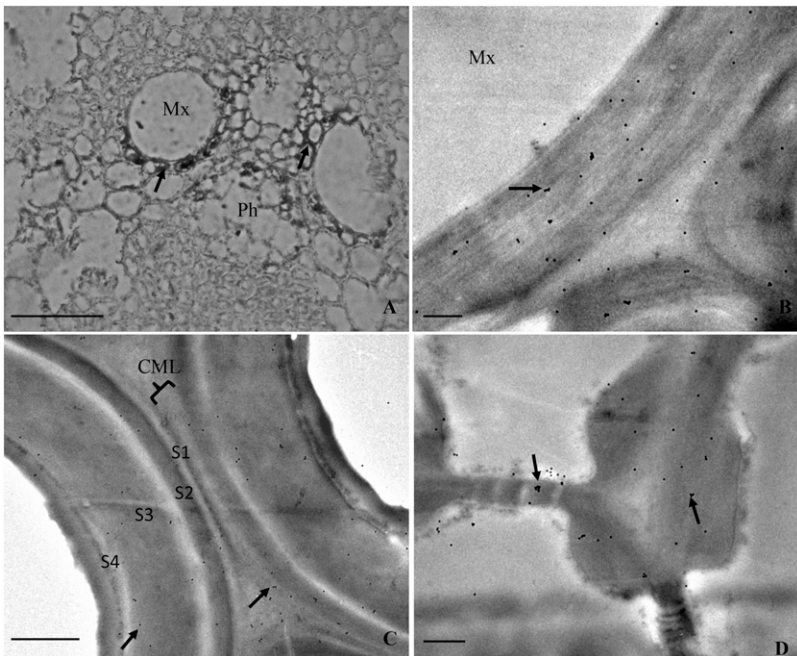


Fig. 6. Localization of indole-3-acetic acid (IAA) in internode 1 of 3-month-old *Fargesia yunnanensis* culms. The young culms completed their vertical growth. (A) Immunohistochemical localization of IAA in transverse sections of vascular bundles revealed additional strong signals in cells surrounding the vascular tissues (black arrows); Mx = metaxylem, Ph = phloem; bar = 20  $\mu$ m. (B) A large number of gold particles were localized in metaxylem walls (black arrows); bar = 0.5  $\mu$ m. (C) A large number of gold particles were also observed in fiber walls (black arrows). Four layers of secondary wall (S1, S2, S3, and S4) were deposited; CML = compound middle lamella, bar = 1  $\mu$ m. (D) Many gold particles were localized in parenchymal cell walls (black arrows); bar = 0.5  $\mu$ m.

the mature bamboo through the rhizome to sustain their rapid growth (Su, 1965). Song et al. (2016) also reported that almost all carbohydrates in leaves, branches, and trunks are transferred to the growing shoots. Therefore, the translocation of both water and the flow of photoassimilates should be acropetal in fast-elongating shoots, which are mainly supplied by the attached mature bamboos. Hence, if the nonfunctional shoot apex could synthesize auxin, the hormone is unlikely to move into the basal internodes over a long distance against the stream of water and photoassimilates in the xylem and phloem. Therefore, it is more reasonable that the high concentration of

IAA in the shoot apex has been transported from the attached mature bamboos. Furthermore, there is no apical dominance in bamboo shoots until the branches and leaves have sprouted. In recent years, some researchers have proposed that IAA is transported to, rather than produced in, the shoot apical stem through the vascular tissues (Aloni, 2001; Avsian-Kretschmer et al., 2002; Hou and Huang, 2005). The results of the current study support this hypothesis.

A higher rate of parenchymal cell division and more intense IAA signals were observed in the unelongated internodes compared with the rapidly elongating internodes of 0.5-month-old shoots. However, the elongation of parenchymal cells, i.e., the formation of long and short cells, was the main characteristic of the rapidly elongating internodes, in which a faint IAA signal was detected. These results suggested that IAA participated in the mediation of parenchymal cell division in unelongated internodes but not in cell elongation. Wang et al. (2015) also reported that cell length was not correlated to the IAA concentration, but it correlated positively to IAA/ABA. In tomato (*Solanum lycopersicum*), the IAA-induced fruit remains smaller than the seeded control fruit but has a similar number of cells, whereas the pericarp of the gibberellin-induced fruit contains fewer cells but has a larger volume than the seeded fruit (Bünger-Kibler and Bangerth, 1982). These findings indicate that IAA and gibberellin lead to an increased number of cells and cell expansion, respectively (de Jong et al., 2009). Yang et al. (2003) also reported a significant correlation between IAA and the rate of cell division. Javid et al. (2011) also considered that auxin may stimulate cell division. Therefore, the unelongated internodes had more IAA than the rapidly elongating internodes.

The immunohistochemical localization revealed a strong IAA signal in vascular tissues, including those cells surrounding vascular elements and companion cells in the phloem. In addition, the parenchymal cells between vascular bundles and between the xylem and phloem also displayed a strong IAA signal. These results suggested that IAA was transported in vascular bundles and then unloaded and stored in parenchymal cells. Ruegger et al. (1997) proposed that continuous auxin transport is necessary for the formation of vascular bundles. Auxin is important for the induction of vascular tissue development (Sieburth, 1999). Dong et al. (2012) also reported an accumulation of IAA in the vascular bundles of basal regions of the leaf petioles of hybrid poplar 'Poplar 741' [*Populus alba*  $\times$  (*Populus davidiana* + *Populus simonii*)  $\times$  *Populus tomentosa*]. However, a new study showed the opposite results, demonstrating only a weak IAA signal in vascular bundles, but strong signals in the cells

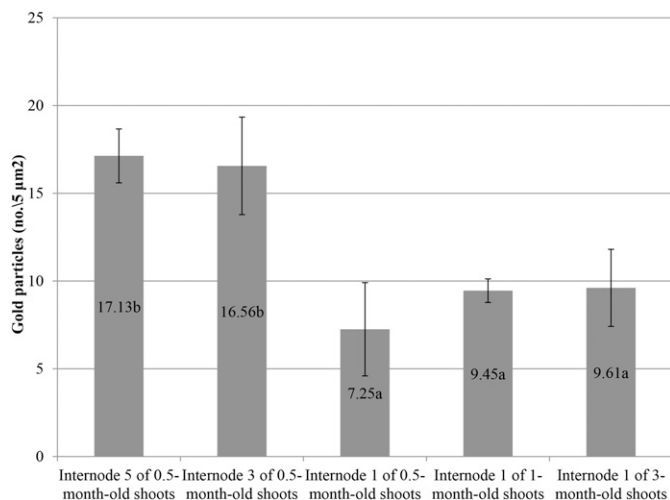


Fig. 7. Density of the gold particles in parenchymal cells during internode development of *Fargesia yunnanensis* shoots and culms. Values are expressed as the mean number of gold particles (no./5 μm<sup>2</sup>). Means with the same letters were not significantly different. The density of the gold particles decreased significantly with rapid internode elongation, and then slightly increased upon completion of elongation of the internode and vertical growth of the culm.

surrounding the vascular tissues in peach (*Prunus persica*; Zhang et al., 2015).

According to the subcellular localization of endogenous IAA during shoot internode elongation, the internode development process could be divided into two developmental stages, i.e., the differentiation and elongation stage and the maturation stage. During the differentiation and elongation stage, IAA signals were mainly localized in the cytoplasm and nuclei; very little signal was detected in the vacuoles and cell walls. During internode elongation, the vacuoles enlarged and pressed the cytoplasm against the cell wall in parenchymal and fiber cells. Hence, a strong IAA signal was also detected in the vicinity of cell walls. After internode elongation, the internode began to mature, and very little cytoplasm or nuclei could be detected in fiber and parenchymal cells. Secondary wall deposition also occurred in parenchymal and fiber cell walls based on ultramicroscopic observations. A large number of gold particles were detected in fiber and parenchymal cell walls. These observations were supported by the statistical data for the immunogold particle density, i.e., the density of immunogold particles increased slightly after the completion of internode elongation.

Dong et al. (2014) reported that the distribution of IAA in the plasma membrane and nucleus suggests a physiological activity

of IAA during leaf rhizogenesis of hybrid poplar 'Poplar 741'. The IAA signals in nuclei might be related to a multitude of different developmental and physiological activities during cell division and elongation in bamboo internodes. The distribution of IAA in the cytoplasm may represent intracellular auxin homeostasis of IAA signal transduction, transport, and metabolism. In maize (*Zea mays*) coleoptile tips, IAA also has been reported to be localized in the cytoplasm, plastids, and mitochondria, but not in the vacuoles and cell walls (Nishimura et al., 2011). A similar trend has also been observed in fiber and parenchymal cells before the cessation of internode elongation, with very little IAA signal detected in cell walls. Previous studies have demonstrated that high concentrations of IAA induce short fibers with thick secondary walls, whereas high levels of GA result in long fibers with thin secondary walls (Aloni, 1979; Aloni et al., 1990; Roberts et al., 1988). In the present study, an increase in IAA signals was detected in cell walls after internode elongation, showing that IAA might be positively related to secondary wall deposition in both parenchymal and fiber cells. However, this hypothesis requires further confirmation.

**LOCALIZATION OF ABA AND INTERNODE ELONGATION.** In this study, immunofluorescence revealed the

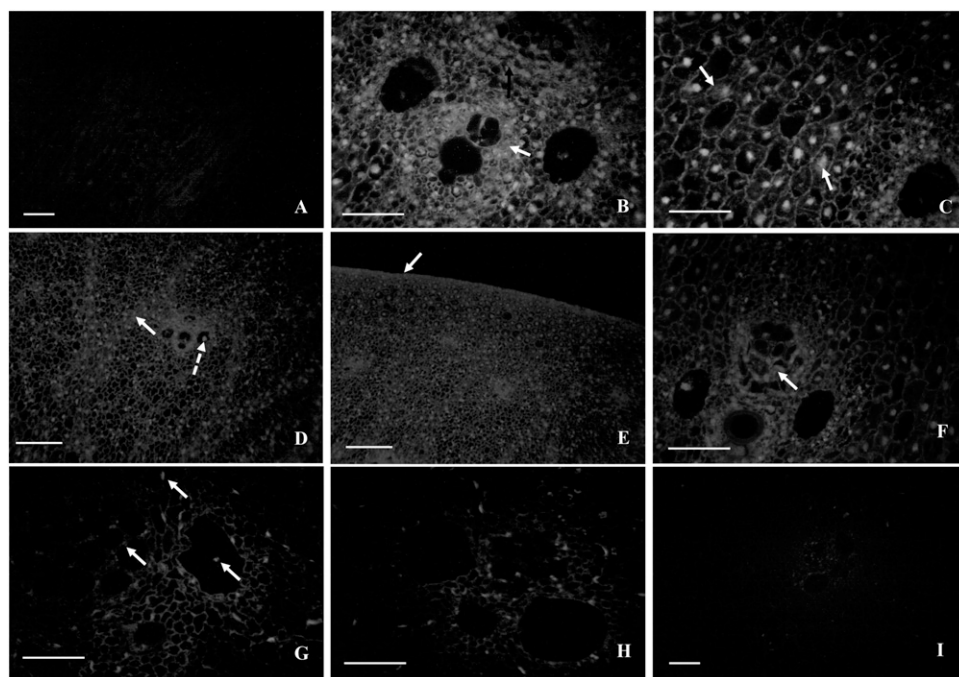


Fig. 8. Immunofluorescence localization of abscisic acid (ABA) in different internodes of *Fargesia yunnanensis* shoots and culms: (A) longitudinal section and (B–J) transverse section; bar = 20 μm. (A) A longitudinal section of the shoot apex showing a faint ABA signal. (B) The vascular bundle of internode 5 of 0.5-month-old shoots, showing a strong signal in the parenchymal and fiber cells surrounding the vascular tissues (white arrow) and companion cells in the phloem (dotted arrow). (C) The parenchymal cells between the vascular bundles in internode 5 of 0.5-month-old shoots displayed strong signals in the cytoplasm (white arrows) and nuclei. (D–F) Immunofluorescence localization of ABA in internode 3 of 0.5-month-old shoots (elongation initiated), showing that the ABA signal (white arrows) was mainly detected in the parenchymal cells between (D) vascular bundles, (E) culm skin, and (F) companion cells. ABA signal (dotted arrow) was also observed in the cytoplasm of metaxylem vessels, but it was weaker than that in internode 5. (G) The ABA signal in the elongating internode 1 of 0.5-month-old shoots, which was mainly detected in cells surrounding vascular tissues, companion cells, and parenchymal cell nuclei between the metaxylem and phloem. The ABA signal could also be detected in the residual cytoplasm of the metaxylem. (H) The ABA signal in internode 1 of 1-month-old shoots, revealing an even weaker signal. (I) The ABA signal could barely be detected in internode 1 of 3-month-old culms.

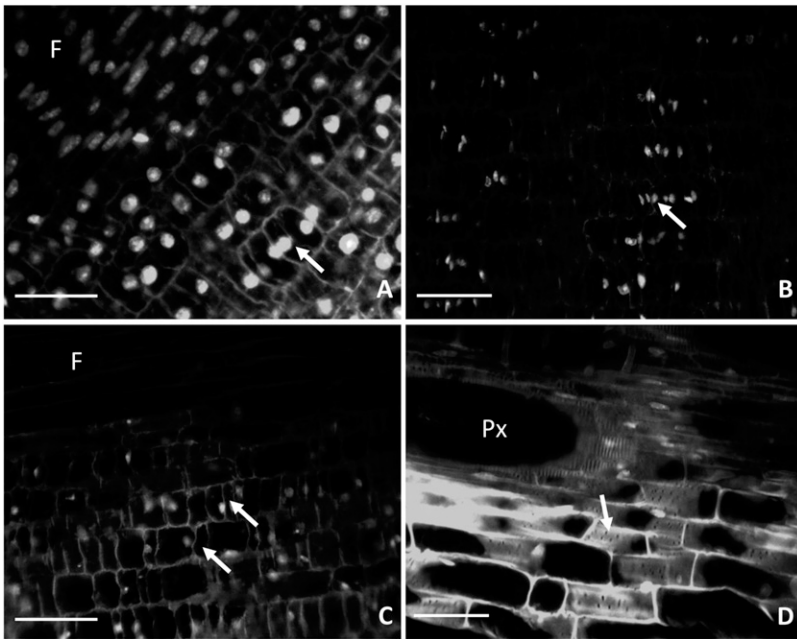


Fig. 9. Anatomical observations of longitudinal sections of different internodes from *Fargesia yunnanensis* shoots; bar = 20  $\mu$ m. (A) An internode close to the shoot apex, showing prominent nuclei in both parenchymal and fiber cells. Fiber elongation and parenchymal cell division (white arrow) could be observed, but the internode did not elongate significantly during this period; F = fiber. (B) An unelongated internode (internode 5 of 0.5-month-old shoots), showing that some parenchymal cell nuclei adjoined one another, as indicated by the rapid cell division during this stage. (C) The rapidly elongating internode 1 of 0.5-month-old shoots, showing the formation of long and short cells (white arrows). Nuclei were observed in a few parenchymal cells. (D) Internode 1 of 1-month-old shoots with cessation of internode elongation. Long- and short-cell formation. Significant pits (white arrow) in the lateral walls suggested deposition of the secondary cell wall.

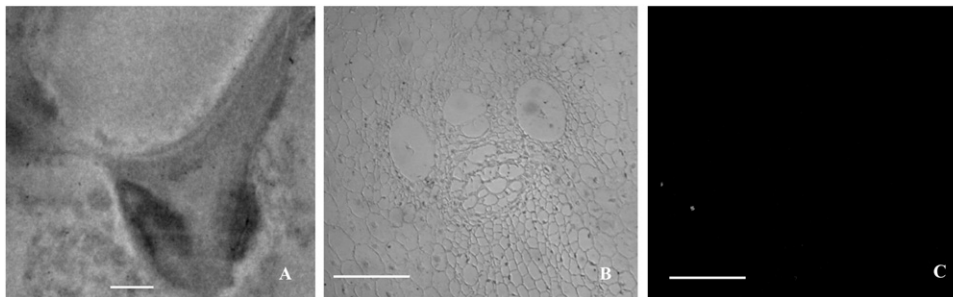


Fig. 10. Controls for the immunochemical localization of indole-3-acetic acid (IAA) and abscisic acid (ABA) in internode 1 of *Fargesia yunnanensis* shoots. (A and B) No IAA signals were detected in ultrathin or paraffin sections in the absence of the primary anti-IAA antibody; (A) bar = 0.5  $\mu$ m, (B) bar = 20  $\mu$ m. (C) No ABA signals were detected in the sections in the absence of the primary anti-IAA antibody; bar = 20  $\mu$ m.

strongest ABA signals in the unelongated internode of 0.5-month-old shoots. On initiation of internode elongation, the signal began to weaken, with the weakest signals observed in the internodes of 3-month-old shoots. These results suggested that ABA was negatively related to internode elongation. Although the strongest signals were detected in the unelongated internode, considerable parenchymal cell divisions could still be observed, indicating that the unelongated internode was still differentiating. A similar relationship between ABA levels and the developmental stage of the tissues has also been observed in other plant species. For example, the

highest ABA levels were found in immature leaves and buds, with lower levels occurring in mature leaves (Thorsteinsson et al., 1990; Zeevaart and Boyer, 1984). Current theory suggests that ABA is a “negative” growth regulator and that its accumulation is associated with stress responses and dormancy (Grill and Himmelbach, 1998; Peng et al., 2006). However, the latest research findings have demonstrated a “positive” role of ABA in plants (Peng et al., 2006). Liso et al. (1984) first reported that ABA is required for cell division. Previous studies have shown that cell cycle progression is blocked in G1 when the ABA content of actively proliferating cells of the root apex are experimentally lowered, and cell division is stimulated when the ABA content is raised (Arrigoni et al., 1997; Citterio et al., 1994). It has also been reported that ABA not only stimulates cell proliferation in the meristem but also induces new DNA synthesis in 80% of quiescent center cells (Innocenti et al., 1990; Liso et al., 1988). The results of the present study support the hypothesis that ABA is required for cell division but not for cell elongation. On completion of internode elongation, parenchymal cell division ceased, and very little ABA signal could be detected.

Strong signals appeared in parenchymal cells between vascular bundles and between vascular elements, cortical cells, and those cells surrounding vascular elements, implying that those cells were involved in the transportation and storage of ABA. Similar findings have also been reported for maize roots (Schraut et al., 2004). The ABA in the cytoplasm and nuclei of parenchymal cells might be related to intracellular transportation, signal transduction, and perception. The strong ABA signal detected in cell walls might be related to extracellular and intercellular transportation. Schraut et al. (2004) also reported that the strongest ABA-specific signals originated from cell walls together with the cytoplasmic layer. A strong ABA signal was also observed in

the companion cells of the phloem, which was similar to the distribution of IAA. This similarity might be related to the unloading of endogenous hormones. However, Peng et al. (2003) considered the localization of ABA in phloem cells to be due to regulation of the flow and distribution of assimilates. In addition, few ABA signals could be detected in the shoot apex, which was significantly different from the distribution of IAA.

In conclusion, the strongest IAA and ABA signals, together with anatomical observations for unelongated internodes, suggested that both hormones participated in the mediation

of internode differentiation, but not in the rapid internode elongation. Moreover, IAA was also involved in secondary cell wall deposition in both parenchymal and fiber cells.

### Literature Cited

- Aloni, R. 1979. Role of auxin and gibberellin in differentiation of primary phloem fibers. *Plant Physiol.* 63:609–614.
- Aloni, R., M.T. Tollier, and B. Monties. 1990. The role of auxin and gibberellin in controlling lignin formation in primary phloem fibers and in xylem of *Coleus blumei* stems. *Plant Physiol.* 94:1743–1747.
- Aloni, R. 2001. Foliar and axial aspects of vascular differentiation: Hypotheses and evidence. *J. Plant Growth Regulat.* 20:22–34.
- Arenas-Huertero, F., A. Arroyo, L. Zhou, J. Sheen, and P. Leon. 2000. Analysis of *Arabidopsis* glucose insensitive mutants, *gin5* and *gin6*, reveals a central role of the plant hormone ABA in the regulation of plant vegetative development by sugar. *Genes Dev.* 14:2085–2096.
- Arrigoni, O., G. Calabrese, L. De Gara, M.B. Bitonti, and R. Liso. 1997. Correlation between changes in cell ascorbate and growth of *Lupinus albus* seedlings. *J. Plant Physiol.* 150:302–308.
- Avsian-Kretchmer, O., J.C. Cheng, L. Chen, E. Moctezuma, and Z.R. Sung. 2002. Indole acetic acid distribution coincides with vascular differentiation pattern during *Arabidopsis* leaf ontogeny. *Plant Physiol.* 130:199–209.
- Brocard-Gifford, I., T.J. Lynch, M.E. Garcia, B. Malhotra, and R.R. Finkelstein. 2004. The *Arabidopsis thaliana* ABSCISIC ACID-INSENSITIVE8 locus encodes a novel protein mediating abscisic acid and sugar responses essential for growth. *Plant Cell* 16:406–421.
- Bünger-Kibler, S. and F. Bangerth. 1982. Relationship between cell number, cell size and fruit size of seeded fruit of tomato (*Lycopersicon esculentum* Mill.), and those induced parthenocarpically by the application of plant growth regulators. *Plant Growth Regulat.* 1:143–154.
- Çakir, B., A. Agasse, C. Gaillard, A. Saumonneau, S. Delrot, and R. Atanassova. 2003. A grape ASR protein involved in sugar and abscisic acid signaling. *Plant Cell* 15:2165–2180.
- Carrari, F., A.R. Fernie, and N.D. Iusem. 2004. Heard it through the grapevine? ABA and sugar cross-talk: The ASR story. *Trends Plant Sci.* 9:57–59.
- Chen, D., Y. Ren, Y. Deng, and J. Zhao. 2010. Auxin polar transport is essential for the development of zygote and embryo in *Nicotiana tabacum* L. and correlated with ABP1 and PM H<sup>+</sup>-ATPase activities. *J. Expt. Bot.* 61:1853–1867.
- Chudasama, R.S. and V. Thaker. 2007. Free and conjugated IAA and PAA in developing seeds of two varieties of pigeon pea (*Cajanus cajan*). *Gen. Appl. Plant Physiol.* 33:41–57.
- Citterio, S., S. Sgorbati, S. Scippa, and E. Sparvoli. 1994. Ascorbic acid effect on the onset of cell proliferation in pea root. *Physiol. Plant.* 92:601–607.
- Cui, K., C.Y. He, J.G. Zhang, A.G. Duan, and Y.F. Zeng. 2012. Temporal and spatial profiling of internode elongation-associated protein expression in rapidly growing culms of bamboo. *J. Proteome Res.* 11:2492–2507.
- de Jong, M., C. Mariani, and W.H. Vriezen. 2009. The role of auxin and gibberellin in tomato fruit set. *J. Expt. Bot.* 60:1523–1532.
- Ding, X.C. 1997. Dynamic analysis for endogenous phytohormones of bamboo shoots (*Phyllostachys heterocycla* var. *pubescens*) during different growth and differentiation stage. *J. Bamboo Res.* 16:53–62.
- Dong, N., Y. Gao, Y. Hao, W. Yin, and D. Pei. 2014. Subcellular localization of endogenous IAA during poplar leaf rhizogenesis revealed by in situ immunocytochemistry. *Plant Biotechnol. Rpt.* 8:377–386.
- Dong, N., D. Pei, and W. Yin. 2012. Tissue-specific localization and dynamic changes of endogenous IAA during poplar leaf rhizogenesis revealed by in situ immunohistochemistry. *Plant Biotechnol. Rpt.* 6:165–174.
- Dulbecco, R. and M. Vogt. 1954. Plaque formation and isolation of pure lines with poliomyelitis viruses. *J. Exp. Med.* 99:167–182.
- Elbaz, M., A. Avni, and M. Weil. 2002. Constitutive caspase-like machinery executes programmed cell death in plant cells. *Cell Death Differ.* 9:726–733.
- Falasca, G., D. Zaghi, M. Possenti, and M.M. Altamura. 2004. Adventitious root formation in *Arabidopsis thaliana* thin cell layers. *Plant Cell Rpt.* 23:17–25.
- Finkelstein, R.R. and S.I. Gibson. 2002. ABA and sugar interactions regulating development: Cross-talk or voices in a crowd? *Curr. Opin. Plant Biol.* 5:26–32.
- Gangopadhyay, M., D. Chakraborty, S. Dewanjee, and S. Bhattacharya. 2010. Clonal propagation of *Zephyranthes grandiflora* using bulbs as explants. *Biol. Plant.* 54:793–797.
- Gorpenchenko, T.Y., D.L. Aminin, Y.V. Vereshchagina, Y.N. Shkryl, G.N. Veremeichik, G.K. Tchernoded, and V.P. Bulgakov. 2012. Can plant oncogenes inhibit programmed cell death? *Plant Signal. Behav.* 7:1058–1061.
- Grill, E. and A. Himmelbach. 1998. ABA signal transduction. *Curr. Opin. Plant Biol.* 1:412–418.
- Gubler, F., A.A. Millar, and J.V. Jacobsen. 2005. Dormancy release, ABA and pre-harvest sprouting. *Curr. Opin. Plant Biol.* 8:183–187.
- Hou, Z.X. and W.D. Huang. 2005. Immunohistochemical localization of IAA and ABP1 in strawberry shoot apices during floral induction. *Planta* 222:678–687.
- Innocenti, A.M., M.B. Bitonti, O. Arrigoni, and R. Liso. 1990. The size of quiescent centre in roots of *Allium cepa* L. grown with ascorbic acid. *New Phytol.* 114:507–509.
- Jaillais, Y. and J. Chory. 2010. Unraveling the paradoxes of plant hormone signaling integration. *Nat. Struct. Mol. Biol.* 17:642–645.
- Javid, M.G., A. Sorooshzadeh, S.A.M.M. Sanavy, I. Allahdadi, and F. Moradi. 2011. Effects of the exogenous application of auxin and cytokinin on carbohydrate accumulation in grains of rice under salt stress. *Plant Growth Regulat.* 65:305–313.
- Liese, W. and M. Köhl (eds.). 2015. Bamboo: The plant and its uses. Springer, Cham, Switzerland.
- Liso, R., G. Calabrese, M.B. Bitonti, and O. Arrigoni. 1984. Relationship between ascorbic acid and cell division. *Expt. Cell Res.* 150:314–320.
- Liso, R., A.M. Innocenti, M.B. Bitonti, and O. Arrigoni. 1988. Ascorbic acid-induced progression of quiescent centre cells from G1 to S phase. *New Phytol.* 110:469–471.
- Ljung, K., R.P. Bhalerao, and G. Sandberg. 2001. Sites and homeostatic control of auxin biosynthesis in *Arabidopsis* during vegetative growth. *Plant J.* 28:465–474.
- Ludwig-Muller, J., A. Vertocnik, and C.D. Town. 2005. Analysis of indole-3-butyric acid-induced adventitious root formation on *Arabidopsis* stem segments. *J. Expt. Bot.* 56:2095–2105.
- Magel, E., S. Kruse, G. Lütje, and W. Liese. 2005. Soluble carbohydrates and acid invertases involved in the rapid growth of developing culms in *Sasa palmata* (bean). *Camus. Bamboo Sci. Cult.* 19:23–29.
- Mano, Y. and K. Nemoto. 2012. The pathway of auxin biosynthesis in plants. *J. Expt. Bot.* 63:2853–2872.
- Mauch-Mani, B. and F. Mauch. 2005. The role of abscisic acid in plant–pathogen interactions. *Curr. Opin. Plant Biol.* 8:409–414.
- Moore, T.C. 1989. Biochemistry and physiology of plant hormones. Springer-Verlag, New York, NY.
- Nishimura, T., K. Toyooka, M. Sato, S. Matsumoto, M.M. Lucas, M. Strnad, F. Baluska, and T. Koshiba. 2011. Immunohistochemical observation of indole-3-acetic acid at the IAA synthetic maize coleoptile tips. *Plant Signal. Behav.* 6:2013–2022.
- Opaskornkul, C., S. Lindberg, and J.E. Tilberg. 1999. Effect of ABA on the distribution of sucrose and protons across the plasmalemma of pea mesophyll protoplasts—Suggesting a sucrose/proton symport. *J. Plant Physiol.* 154:447–453.
- Peng, Y.B., Y.F. Lu, and D.P. Zhang. 2003. Abscisic acid activates ATPase in developing apple fruit especially in fruit phloem cells. *Plant Cell Environ.* 26:1329–1342.
- Peng, Z., Y. Lu, L. Li, Q. Zhao, Q. Feng, Z. Gao, H. Lu, T. Hu, N. Yao, K. Liu, Y. Li, D. Fan, Y. Guo, W. Li, Y. Lu, Q. Weng, C. Zhou,

- L. Zhang, T. Huang, Y. Zhao, C. Zhu, X. Liu, X. Yang, T. Wang, K. Miao, C. Zhuang, X. Cao, W. Tang, G. Liu, Y. Liu, J. Chen, Z. Liu, L. Yuan, Z. Liu, X. Huang, T. Lu, B. Fei, Z. Ning, B. Han, and Z. Jiang. 2013. The draft genome of the fast-growing non-timber forest species moso bamboo (*Phyllostachys heterocycla*). *Nat. Genet.* 45:456–461.
- Peng, Y.B., C. Zou, D.H. Wang, H.Q. Gong, Z.H. Xu, and S.N. Bai. 2006. Preferential localization of abscisic acid in primordial and nursing cells of reproductive organs of *Arabidopsis* and cucumber. *New Phytol.* 170:459–466.
- Roberts, L.W., B.P. Gahan, and R. Aloni. 1988. *Vascular differentiation and plant growth regulators*. Springer-Verlag, Berlin, Germany.
- Rock, C.D. and X. Sun. 2005. Crosstalk between ABA and auxin signaling pathways in roots of *Arabidopsis thaliana* (L.) Heynh. *Planta* 222:98–106.
- Rook, F., F. Corke, R. Card, G. Munz, C. Smith, and M.W. Bevan. 2001. Impaired sucrose-induction mutants reveal the modulation of sugar-induced starch biosynthetic gene expression by abscisic acid signaling. *Plant J.* 26:421–433.
- Ruegger, M., E. Dewey, L. Hobbie, D. Brown, P. Bernasconi, J. Turner, G. Muday, and M. Estelle. 1997. Reduced naphthylphthalamic acid binding in the tir3 mutant of *Arabidopsis* is associated with a reduction in polar auxin transport and diverse morphological defects. *Plant Cell* 9:745–757.
- Santner, A. and M. Estelle. 2009. Recent advances and emerging trends in plant hormone signaling. *Nature* 459:1071–1078.
- Schraut, D., C.I. Ullrich, and W. Hartung. 2004. Lateral ABA transport in maize roots (*Zea mays*): Visualization by immunolocalization. *J. Expt. Bot.* 55:1635–1641.
- Sieburth, L.E. 1999. Auxin is required for leaf vein pattern in *Arabidopsis*. *Plant Physiol.* 121:1179–1190.
- Smeeckens, S. 2000. Sugar-induced signal transduction in plants. *Annu. Rev. Plant Biol.* 51:49–81.
- Song, X., C. Peng, G. Zhou, H. Gu, Q. Li, and C. Zhang. 2016. Dynamic allocation and transfer of non-structural carbohydrates, a possible mechanism for the explosive growth of Moso bamboo (*Phyllostachys heterocycla*). *Sci. Rpt.* 6:1–8.
- Su, J.C. 1965. Carbohydrate metabolism in shoots of bamboo *Leleba oldhami*. I. Preliminary survey of soluble saccharides and sucrose-degrading enzymes. *Bot. Bull. Acad. Sin.* 6:153–159.
- Teale, W.D., I.A. Paponov, and K. Palme. 2006. Auxin in action: Signaling, transport and the control of plant growth and development. *Nat. Rev. Mol. Cell Biol.* 7:847–859.
- Thomas, C., R. Bronner, J. Molinier, E. Prinsen, H. van Onckelen, and G. Hahne. 2002. Immuno-cytochemical localization of indole-3-acetic acid during induction of somatic embryogenesis in cultured sunflower embryos. *Planta* 215:577–583.
- Thorsteinsson, B., E. Tillberg, and T. Ericsson. 1990. Levels of IAA, ABA and carbohydrates in source and sink leaves of *Betula pendula* Roth. Effects of varying the relative rate of nutrient addition. *Scand. J. For. Res.* 5:347–354.
- Verslues, P.E. and J.K. Zhu. 2005. Before and beyond ABA: Upstream sensing and internal signals that determine ABA accumulation and response under abiotic stress. *Biochem. Soc. Trans.* 33:375–379.
- Vieten, A., M. Sauer, P.B. Brewer, and J. Friml. 2007. Molecular and cellular aspects of auxin-transport-mediated development. *Trends Plant Sci.* 12:160–168.
- Wang, H.Y., K. Cui, C.Y. He, Y.F. Zeng, S.X. Liao, and J.G. Zhang. 2015. Endogenous hormonal equilibrium linked to bamboo culm development. *Genet. Mol. Res.* 14:11312–11323.
- Wang, S., Y. Ding, S. Lin, X. Ji, and H. Zhan. 2016. Seasonal changes of endogenous soluble sugar and starch in different developmental stages of *Fargesia yunnanensis*. *J. Wood Sci.* 62:1–11.
- Woodward, A.W. and B. Bartel. 2005. Auxin: Regulation, action, and interaction. *Ann. Bot. (Lond.)* 95:707–735.
- Xuan, W., F.Y. Zhu, S. Xu, B.K. Huang, T.F. Ling, J.Y. Qi, M.B. Ye, and W.B. Shen. 2008. The heme oxygenase/carbon monoxide system is involved in the auxin-induced cucumber adventitious rooting process. *Plant Physiol.* 148:881–893.
- Yamaguchi-Shinozaki, K. and K. Shinozaki. 2005. Organization of cis-acting regulatory elements in osmotic- and cold-stress-responsive promoters. *Trends Plant Sci.* 10:88–94.
- Yang, J., J. Zhang, Z. Wang, and Q. Zhu. 2003. Hormones in the grains in relation to sink strength and postanthesis development of spikelets in rice. *Plant Growth Regulat.* 41:185–195.
- Zeevaart, J.A. and G.L. Boyer. 1984. Accumulation and transport of abscisic acid and its metabolites in *Ricinus* and *Xanthium*. *Plant Physiol.* 74:934–939.
- Zhang, D.P., C. Huang, and W. Jia. 1999. Immunogold electron-microscopy localization of abscisic acid in flesh cells of grape berry (*Vitis vinifera* L. × *Vitis labrusca* L. cv Kyoho). *Sci. Hort.* 81:189–198.
- Zhang, D.P., S.W. Chen, Y.B. Peng, and Y.Y. Shen. 2001a. Abscisic acid-specific binding sites in the flesh of developing apple fruit. *J. Expt. Bot.* 52:2097–2103.
- Zhang, W., Y. Li, M. Shi, H. Hu, B. Hua, A. Yang, and Y. Liu. 2015. Immunohistochemical localization of endogenous IAA in peach (*Prunus persica* L.) fruit during development. *Korean J. Hort. Sci. Technol.* 33:317–325.
- Zhang, D.P., Y.M. Lu, Y.Z. Wang, C.Q. Duan, and H.Y. Yan. 2001b. Acid invertase is predominantly localized to cell walls of both the practically symplasmically isolated sieve element/companion cell complex and parenchyma cells in developing apple fruit. *Plant Cell Environ.* 24:691–702.